Physics Faculty Publications   Department of Physics

1-1-2008

Local Structures Surrounding Zr in Nanostructurally Stabilized Cubic Zirconia: Structural Origin of Phase Stability

Y. L. Soo
National Tsing Hua University, Taiwan, soo@phys.nthu.edu.tw

P. J. Chen
National Tsing Hua University, Taiwan

S. H. Huang
National Tsing Hua University, Taiwan

T. J. Shiu
National Tsing Hua University, Taiwan

T Y. Tsai
National Tsing Hua University, Taiwan

Authors

Y. L. Soo; P. J. Chen; S. H. Huang; T. J. Shiu; T Y. Tsai; Y. H. Chow; Y. C. Lin; S. C, Weng; S. L. Chang; G. Wang; Chin Li Cheung; Renat F. Sabirianov; Wai-Ning Mei; Fereydoon Namavar; Hani Haider; Kevin L. Garvin; J. F. Lee; H. Y. Lee; and P. P. Chu

1-1-2008

Local Structures Surrounding Zr in Nanostructurally Stabilized Cubic Zirconia: Structural Origin of Phase Stability

Y. L. Soo
National Tsing Hua University, Hsinchu 30013, Taiwan

P. J. Chen
National Tsing Hua University, Hsinchu 30013, Taiwan

S. H. Huang
National Tsing Hua University, Hsinchu 30013, Taiwan

T. J. Shiu
National Tsing Hua University, Hsinchu 30013, Taiwan

T. Y. Tsai
National Tsing Hua University, Hsinchu 30013, Taiwan

See next page for additional authors

Recommended Citation

Authors

Y. L. Soo, P. J. Chen, S. H. Huang, T. J. Shiu, T. Y. Tsai, Y. H. Chow, S. C. Weng, Y. C. Lin, S. L. Chang, G. Wang, Chin Li Cheung, R. F. Sabirianov, W. N. Mei, F. Namavar, H. Haider, K. L. Garvin, J. F. Lee, H. Y. Lee, and P. P. Chu

Local structures surrounding Zr in nanostructurally stabilized cubic zirconia: Structural origin of phase stability

Y. L. Soo,[1,a] P. J. Chen,[1] S. H. Huang,[1] T. J. Shiu,[1] T. Y. Tsai,[1] Y. H. Chow,[1] Y. C. Lin,[1] S. C. Weng,[1] S. L. Chang,[1] G. Wang,[2] C. L. Cheung,[2] R. F. Sabirianov,[3] W. N. Mei,[3] F. Namavar,[4] H. Haider,[4] K. L. Garvin,[4] J. F. Lee,[5] H. Y. Lee,[6] and P. P. Chu[6]

[1]*Department of Physics, National Tsing Hua University, Hsinchu 30013, Taiwan*
[2]*Department of Chemistry, University of Nebraska-Lincoln, Lincoln, Nebraska 68588, USA*
[3]*Department of Physics, University of Nebraska at Omaha, Omaha, Nebraska 68182, USA*
[4]*Department of Orthopaedics Surgery and Rehabilitation, University of Nebraska Medical Center, Omaha, Nebraska 68198, USA*
[5]*National Synchrotron Radiation Research Center, Hsinchu 30013, Taiwan*
[6]*Department of Chemistry, National Central University, Jhongli 32001, Taiwan*

Local environment surrounding Zr atoms in the thin films of nanocrystalline zirconia (ZrO_2) has been investigated by using the extended x-ray absorption fine structure (EXAFS) technique. These films prepared by the ion beam assisted deposition exhibit long-range structural order of cubic phase and high hardness at room temperature without chemical stabilizers. The local structure around Zr probed by EXAFS indicates a cubic Zr sublattice with O atoms located on the nearest tetragonal sites with respect to the Zr central atoms, as well as highly disordered locations. Similar Zr local structure was also found in a ZrO_2 nanocrystal sample prepared by a sol-gel method. Variations in local structures due to thermal annealing were observed and analyzed. Most importantly, our x-ray results provide direct experimental evidence for the existence of oxygen vacancies arising from local disorder and distortion of the oxygen sublattice in nanocrystalline ZrO_2. These oxygen vacancies are regarded as the essential stabilizing factor for the nanostructurally stabilized cubic zirconia. © *2008 American Institute of Physics.* [DOI: 10.1063/1.3041490]

I. INTRODUCTION

The zirconia (ZrO_2) system has several structural polymorphs such as the cubic, tetragonal, monoclinic, and orthorhombic phases, in which the cubic phase is of most interest in wear-reduction applications due to its high hardness.[1] Without addition of large amount (up to 20%) of trivalent stabilizer oxides such as yttria or ceria, pure zirconia is not normally stable in the cubic phase (diamond simulant) at room temperature.[2] Incorporating these stabilizers in the ZrO_2 sample can generate O vacancies around Zr and therefore stabilize the cubic structure of bulk zirconia.[3] However, the mechanical properties of zirconia deteriorate with increasing concentrations of trivalent stabilizing oxides above 8%.[4] In contrast to bulk ZrO_2, formation of cubic phase without chemical stabilizers has been reported in nanocrystalline zirconia powders with an average grain size of 15 nm.[5–7] In order to prepare adherent hard protective coating for load-bearing applications, nanostructurally stabilized transparent pure (without chemical stabilizer) cubic zirconia films have also been fabricated by using the ion beam assisted deposition (IBAD) technique.[8,9] The IBAD method combines physical vapor deposition with concurrent ion beam bombardment in an ultrahigh vacuum environment to produce films with superior properties that are then "stitched" to substrates such as Si, glass, and metallic medical devices. The measured hardness with nanoindentation[10,11] of nanostructurally stabilized ZrO_2 was up to 16 GPa (Ref. 8) (depending on

deposition conditions), which is significantly larger than a few gigapascals measured for commercially available 21% yttria-stabilized single crystal of cubic zirconia. Furthermore, the as-deposited IBAD samples have demonstrated water contact angles of about $0°-10°$ as compared to those of $50.5° \pm 2.3°$ for cubic zirconia stabilized by a chemical additive.[9] In light of these superior properties, the IBAD-deposited nanocrystalline ZrO_2 films are of great potential in biomedical and other wear-reduction applications and therefore deserve detailed studies.

In order to fully understand the mechanism leading to the stable cubic structure and other physical properties in these nanostructurally stabilized zirconia in the absence of chemical stabilizers, the local structural information pertaining to the bond length variation and structural imperfections is an important prerequisite. To this end, the short-range-order extended x-ray absorption fine structure (EXAFS) technique is a uniquely suitable method. In this paper, we present the EXAFS results on IBAD-fabricated films of nanocrystal ZrO_2, which includes the as-deposited and those annealed at temperatures of 850 and 1000 °C. A nanocrystalline powder sample of ZrO_2 prepared by a *sol-gel* method without hydrolysis is also measured for comparison. Compared with the standard sol-gel process involving hydrolysis, condensation, and polymerization usually adopted for preparing nanocrystal powders of ZrO_2, a process without hydrolysis described in this paper has been found to produce smaller nanoparticles with sizes closer to those in the IBAD samples, and therefore was used in this work.

a)Electronic mail: soo@phys.nthu.edu.tw.
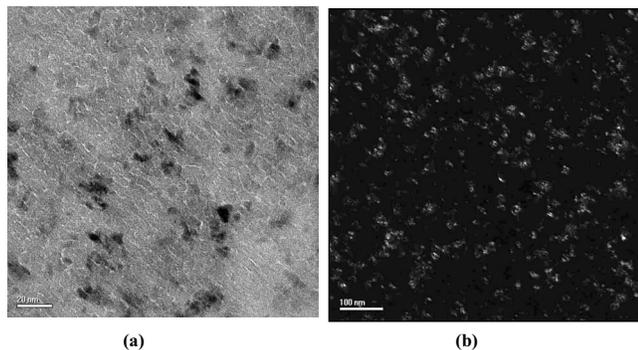
FIG. 1. (a) Bright field and (b) dark field TEM micrographs of the as-deposited IBAD sample. The size range of the crystallites is 5–8 nm.

II. EXPERIMENT

The transparent nanocrystalline ZrO_2 samples reported here were prepared by IBAD at the Nanotechnology Laboratory of the University of Nebraska Medical Center. The IBAD system (Mill Lane Engineering, Lowell, MA) is composed of a Veeco 12 cm rf ion gun that supplies ions at energies up to 1500 eV with a total current density of 500 mA, which provides a broad uniform ion beam of oxygen, nitrogen, and argon and a programable sweep multipocket for electron beam evaporation source. Source material was 99.7% pure white color ZrO_2 with a monoclinic crystal structure from Alfa Aesar (Lot No. C01P41) and was deposited onto silicon, glass, quartz, and metallic substrates. A mixture of O and Ar or N and Ar ion species of ion energy 500 eV was used with evaporation rate around 3 Å/s. Rutherford backscattering spectroscopy (RBS) with 2.275 MeV He^{++} beam was applied to analyze the chemical composition of zirconia films. Electron beam evaporation powder zirconia with concurrent ion beam bombardment and backfill oxygen at room temperature typically resulted in formation of transparent stoichiometric ZrO_2 within accuracy of RBS (4% for oxygen, Evans Analytical Group Sunnyvale, CA). The surface morphology and crystal structure of the ZrO_2 films were characterized by atomic force microscopy, interferometry, x-ray diffractometry (XRD), and transmission electron microscopy (TEM).[8,9]

The as-grown ZrO_2 films deposited on silicon substrates at room temperature and pieces of same ZO_2 samples annealed at 850 and 1000 °C were studied by EXAFS. The grain size distribution of nanocrystals was estimated using TEM micrograph to be about 5–8 nm in diameter (Fig. 1). As shown in Fig. 2, the x-ray diffraction data exhibit cubic phase for the as-deposited and 850 °C-annealed samples. It should be noted that most of the Bragg peaks from the cubic and the tetragonal phases of nanocrystalline ZrO_2 are superimposed partly because of the spreading of peaks due to nanostructures. However, if the tetragonal phase exists in the sample, the (112) peak of tetragonal ZrO_2 at around 43°, as well as splitting of the (400) line of the fluoritelike ZrO_2 structure into (004) and (400) lines with more than one degree of separation, should be observed in the XRD data.[12] As we can see from Fig. 2, none of these important evidences for tetragonal zirconia were observed in samples studied by EXAFS here. By contrast, they were present in the control
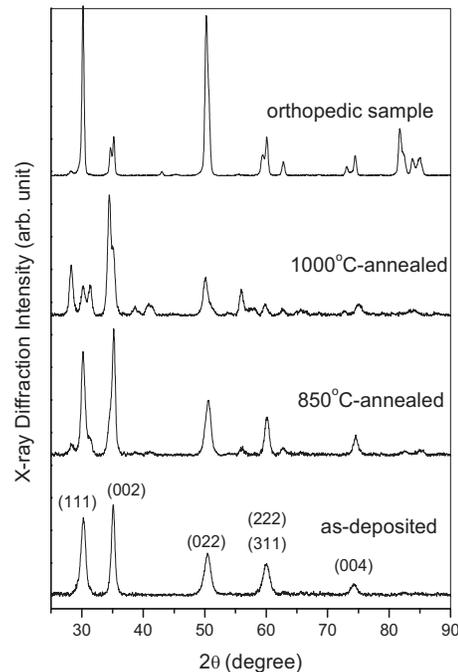
FIG. 2. X-ray diffraction for ZrO_2 samples (from top: orthopedic tetragonal knee ZrO_2, 1000 °C-annealed IBAD ZrO_2, 850 °C-annealed IBAD ZrO_2, and as-deposited IBAD ZrO_2). Curves have been shifted vertically for clarity.

orthopedics knee sample, which is composed of chemically stabilized tetragonal ZrO_2. The possibility of appreciable percentage of tetragonal phase existing in the samples used in this work is therefore excluded. In addition to the cubic peaks, the monoclinic peaks also show up in the XRD of the 1000 °C-annealed sample.

A sol-gel method without hydrolysis was used to prepare a nanocrystal ZrO_2 powder sample for EXAFS measurements. In the sol-gel process, zirconium isopropoxide propanol complex ($Zr \cdot [OCH(CH_3)_2]_4 \cdot (CH_3)_2CHOH$) was used to react with zirconium chloride ($ZrCl_4$) in the presence of trioctylphosphine oxide (TOPO) at an elevated temperature of 340 °C. Zirconium oxide powders were then extracted by a series of washing with acetone and water. The particle size of the sol-gel sample was estimated by XRD data using Scherrer equation to be around 3.6 nm in diameter.

To probe the local structural variation responsible for the enhanced stability in the absence of chemical stabilizer in these nanocrystal samples, the Zr K-edge EXAFS technique was performed on the as-deposited and annealed IBAD samples. The x-ray measurements were carried out in conventional fluorescence mode using an energy dispersive single-element Si(Li) detector at beamline BL01C at Taiwan Light Source (TLS) of National Synchrotron Radiation Research Center (NSRRC) in Taiwan. For comparison, a nanocrystal powder sample of cubic ZrO_2 prepared by a sol-gel method without hydrolysis was also measured.

The EXAFS χ-functions were extracted from the raw experimental data using a well-established data reduction process.[13] The χ as a function of photoelectron momentum (k) was truncated and the curve of χ in between 3.0 and 11.0 Å^{-1} was then Fourier transformed to real (R) space for

TABLE I. Parameters of the local structure around Zr atoms obtained from curve fitting of the Zr K-edge EXAFS. N is the coordination number. R is the bond length. σ^2 is the Debye–Waller-type factor that serves as a measure of local disorder. ΔE_0 is the difference between the zero kinetic energy value of the sample and that of the theoretical model used in FEFF. Uncertainties were estimated by the double-minimum residue ($2\chi^2$) method.

Sample	Neighboring atom	N	R (Å)	σ^2 (10^{-3} Å^2)	ΔE_0 (eV)
Sol-gel	O	3.3 ± 0.6	2.09 ± 0.01	6 ± 2	-8 ± 5
	Zr	12 ± 4	3.62 ± 0.02	10 ± 2	-3 ± 4
IBAD as-deposited	O	4.7 ± 0.7	2.10 ± 0.01	9 ± 2	-8 ± 5
	Zr	13 ± 5	3.59 ± 0.02	14 ± 3	-5 ± 4
IBAD 850 °C-annealed	O	3.2 ± 0.8	2.06 ± 0.01	5 ± 2	-12 ± 5
	Zr	14 ± 5	3.62 ± 0.02	8 ± 2	-4 ± 4
IBAD 1000 °C-annealed	O	5.4 ± 1.0	2.11 ± 0.01	9 ± 2	-8 ± 5
	Zr	14 ± 5	3.43 ± 0.02	12 ± 3	-12 ± 5

direct comparison.[14] To obtain quantitative local structural information, an improved curve-fitting procedure was employed to fit Fourier-filtered functions in k-space[15,16] with theoretical backscattering amplitude and phase-shift functions calculated by the well-known FEFF EXAFS simulation program.[17] The local structural parameters determined by curve fittings are listed in Tables I. The experimental EXAFS χ-functions and Fourier transforms of the as-deposited and the annealed samples, as well as a nanocrystal powder sample prepared by sol-gel method, are plotted with their respective theoretical curve from curve fittings in Figs. 3 and 4, respectively.

III. RESULTS AND DISCUSSION

As shown in Fig. 3, while the χ-function of the as-grown and the 850 °C-annealed IBAD samples are relatively similar to that of the sol-gel sample, that of the 1000 °C-annealed IBAD sample shows distinctly different features especially in the region above 6.0 Å^{-1} indicating larger local structural variation in this sample. The Fourier transforms shown in Fig. 4 exhibit two pronounced peaks for all four ZrO$_2$ samples. The second peak of the 1000 °C-annealed IBAD sample appreciably shifts to the left in comparison to those of other three samples. The local structural parameters listed in Table I obtained from curve-fitting show that the first and the second pronounced peaks represent the nearest (O) shell and the next nearest (Zr) shell from the central Zr atom, respectively. The simplicity of local structures around Zr indicates that the crystal structures of the present samples are mostly close to that in the highly symmetric cubic zirconia structure, which has 8 O nearest neighboring atoms at a distance of 2.20 Å followed by 12 Zr next nearest neighboring atoms at 3.59 Å.[18] However, appreciable deviation from the bulk cubic zirconia structure is observed in these nanocrystal samples. First, the nearest O shell has a much decreased coordination number of around
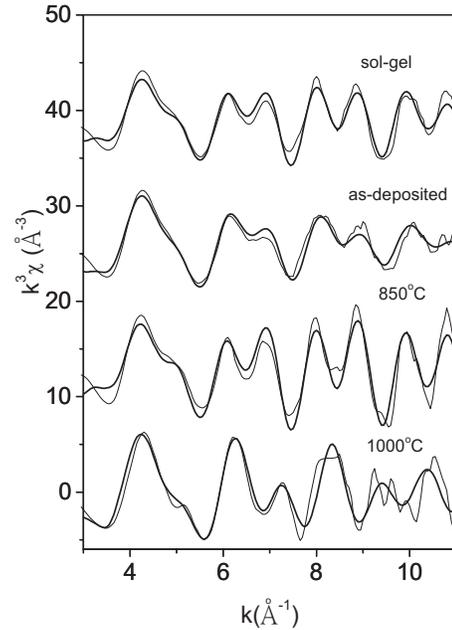
FIG. 3. Weighed Zr K-edge EXAFS χ-functions (from top: sol-gel sample, as-deposited IBAD sample, 850 °C-annealed IBAD sample, and 1000 °C-annealed IBAD sample). Fine lines: experimental; course lines: theoretical. Curves have been shifted vertically for the sake of clarity.

3.2–5.4 in comparison to 8 in the bulk cubic structure. The Zr–O bond length of 2.06–2.11 Å in the nanocrystal samples is also substantially shorter than the bulk value of 2.20 Å. The decreased number of O neighboring atoms surrounding Zr indicates large number of O vacancies in the nanocrystal ZrO$_2$ samples prepared by either the IBAD or the sol-gel method without hydrolysis. Combined with the effect of shortened bondlength, the presence of O vacancies
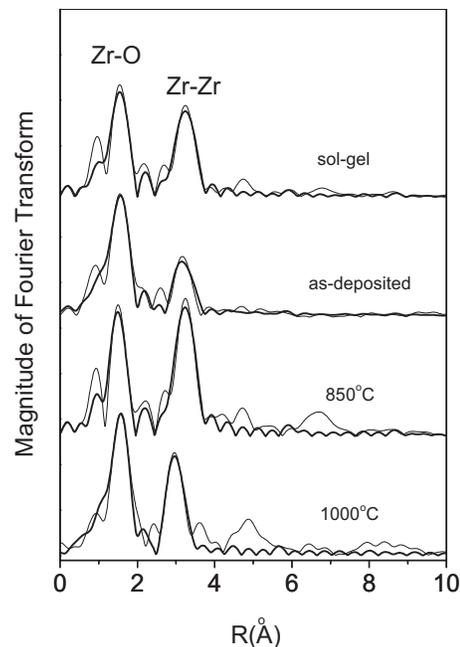
FIG. 4. Fourier transform of Zr K-edge EXAFS χ-functions (from top: sol-gel sample, as-deposited IBAD sample, 850 °C-annealed IBAD sample, and 1000 °C-annealed IBAD sample). Fine lines: experimental; course lines: theoretical. Curves have been shifted vertically for the sake of clarity.
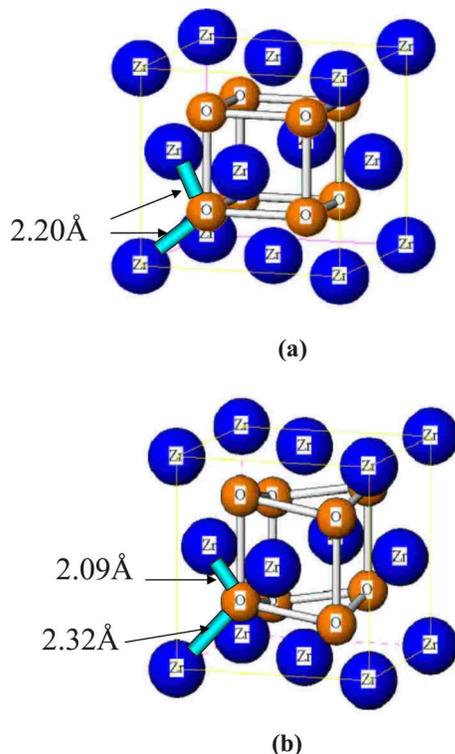
FIG. 5. (Color online) Arrangement of neighboring atoms surrounding Zr in (a) cubic and (b) tetragonal zirconia structures.

has thus stabilized the cubic zirconia structure at room temperature in the nanocrystalline ZrO_2 samples.

It is worth noting that the decreased first-shell (O) coordination number does not necessarily invalidate the measured stoichiometry of nanocrystalline ZrO_2. A large percentage of O atoms may be relocated at the high energy surface of the nanograin boundaries or at interstitial sites with large local structural disorder and thus were not observed by the short-range-order EXAFS technique. The disorderly relocated O atoms can therefore leave behind vacancies at the otherwise cubic/tetragonal oxygen sites. Based on our EXAFS data, it seems reasonable to speculate the following structural model (see Fig. 5): a cubic Zr sublattice with O atoms sitting on tetragonal-like sites relative to the central Zr atoms were formed in the sol gel and the as-deposited IBAD samples. Since the grains are small (3–10 nm) both in the IBAD and sol-gel samples, substantial volume fraction of ZrO_2 is on the surface or intergranular regions where the structure could be disordered. Mediated by the random oxygen vacancy distribution, the disorder may propagate predominantly in the oxygen sublattice and thus diminishes long-range tetragonal order; the soft mode displacement in oxygen sublattice is destroyed. As a result, the zirconia exhibit cubic phase structure observed by XRD measurements. At the same time, oxygen locally occupies tetragonal-like positions, which can be seen from the average Zr–O interactomic distances.

Moreover, while the next nearest (Zr) shell in three of the four nanocrystal samples has coordination numbers and distances similar to those of the bulk cubic zirconia structure, the Zr–Zr distance in the 1000 °C-annealed IBAD sample however dramatically decreases. It is worth noting that the

x-ray diffraction has exhibited a mixed cubic and monoclinic long-range-order structures in the 1000 °C-annealed sample in comparison to the pure-cubic structures in the as-deposited and the 850 °C-annealed samples. Our EXAFS analysis demonstrates substantial change in short-range-order structure at the same annealing temperature of 1000 °C.

As a side remark, we note that Rush *et al.*[19] also reported a much reduced coordination number of 4 for the nearest O shell from the central Zr atom in nanocrystalline zirconia. However, the Zr–O and Zr–Zr distances of 2.13 and 3.41 Å, respectively, in their sample is substantially different from our values of 2.06–2.10 Å and 3.59–3.62 Å for the three pure-cubic-phase samples, respectively. On the other hand, the values 2.11 and 3.43 Å for our 1000 °C-annealed sample, which has a mixed cubic and monoclinic long-range-order structure, are similar to those in their sample. The structures and thermal stability are therefore highly dependent on the different sample preparation methods.

In addition to the most obvious structural differences observed in the 1000 °C-annealed sample, some minor local structural variations are also present among the other three nanocrystal samples. Compared with the sol-gel sample, the as-grown IBAD sample has a larger first-shell coordination number representing less O vacancies in the sample. However, the local disorder represented by the Debye–Waller-type factor (σ^2) in the as-deposited IBAD sample is relatively larger than that in the sol-gel sample for both the first (O) and the second (Zr) shells. Annealing at 850 °C effectively decreases the overall local disorder as well as the first-shell coordination number and substantially shortens the Zr–O bond length in the IBAD sample. When the annealing temperature is increased to 1000 °C, a dramatic local structural variation takes place accompanied by a long-range-order phase transition for an appreciable portion of the materials in the IBAD sample.

IV. CONCLUSIONS

Our EXAFS results have determined the presence of a large amount of O vacancies in cubic ZrO_2 nanocrystal samples prepared by either the IBAD technique or a sol-gel method without hydrolysis. At room temperature, these O vacancies stabilize the cubic structure of nanocrystal zirconia in the absence of chemical stabilizers in the samples. The cubiclike local structure in the IBAD-grown nanocrystal sample is thermally stable up to an annealing temperature of 850 °C. However, when the annealing temperature is raised to 1000 °C, the local environment around Zr undergoes a dramatic change, while the long-range-order crystal structure becomes a mixture of cubic and monoclinic phases. More work has to be performed to obtain a full systematic picture regarding the correlation between particle size, local structure, and long-range-order crystal structure in the nanocrystal ZrO_2 systems. However, our present work has provided a solid experimental evidence for the existence of a large amount of O vacancies in nanostructurally stabilized cubic zirconia. Based on the variation in O coordination number around Zr, our EXAFS results also reveal the dependence of

O vacancies on the sample preparation method and annealing temperature which is very useful for vacancy control in fabricating the nanostructurally stabilized cubic zirconia. Without the need to add chemical stabilizers, the nanocrystal ZrO_2 possesses favorable physical properties compared to the chemically stabilized bulk cubic zirconia and therefore has great potential for many technological applications.

ACKNOWLEDGMENTS

[1] P. Li, I. Wei Chen, and J. E. Penner-Hahn, Phys. Rev. B **48**, 10063 (1993).
[2] C. Piconi and G. Maccauro, Biomaterials **20**, 1 (1999).
[3] P. Li, I. Wei Chen, and J. E. Penner-Hahn, Phys. Rev. B **48**, 10074 (1993).
[4] F. F. Lange, J. Mater. Sci. **17**, 240 (1982).
[5] M. Lajavardi, D. J. Kenney, and S. H. Lin, J. Chin. Chem. Soc. (Taipei) **47**, 1043 (2000).
[6] M. Gateshki, V. Petkov, G. Williams, S. K. Pradhan, and Y. Ren, Phys. Rev. B **71**, 224107 (2005).
[7] P. Bouvier, E. Djurado, G. Lucazeau, and T. Le Bihan, Phys. Rev. B **62**, 8731 (2000).
[8] F. Namavar, G. Wang, C. L. Cheung, R. F. Sabirianov, X. C. Zeng, W. N. Mei, J. Bai, J. R. Brewer, H. Haider, and K. L. Garvin, Nanotechnology **18**, 415702 (2007), and references cited therein.
[9] F. Namavar, C. L. Cheung, R. F. Sabirianov, W. N. Mei, X. C. Zeng, G. Wang, H. Haider, and K. L. Garvin, Nano Lett. **8**, 988 (2008).
[10] W. C. Oliver and G. M. J. Phar, Mater. Res. **7**, 1564 (1992).
[11] M. F. Doerner and W. D. J. Nix, Mater. Res. **1**, 601 (1986).
[12] D. G. Lamas, R. O. Fuentes, I. O. Fabregas, M. E. Fernandez de Rapp, G. E. Lascalea, J. R. Casanova, N. E. Walsoe de Reca, and A. F. Craievich, J. Appl. Crystallogr. **38**, 867 (2005).
[13] M. Newville, P. Lïvins, Y. Yacoby, J. J. Rehr, and E. A. Stern, Phys. Rev. B **47**, 14126 (1993).
[14] P. A. Lee, P. H. Citrin, P. Eisenberger, and B. M. Kincaid, Rev. Mod. Phys. **53**, 769 (1981).
[15] Y. L. Soo, Z. H. Ming, S. W. Huang, Y. H. Kao, R. N. Bhargava, and D. Gallagher, Phys. Rev. B **50**, 7602 (1994), and references cited therein.
[16] Y. L. Soo, S. C. Weng, W. H. Sun, S. L. Chang, W. C. Lee, Y. S. Chang, J. Kwo, M. Hong, J. M. Ablett, C.-C. Kao, D. G. Liu, and J. F. Lee, Phys. Rev. B **76**, 132404 (2007).
[17] J. J. Rehr, J. Mustre de Leon, S. I. Zabinsky, and R. C. Albers, J. Am. Chem. Soc. **113**, 5135 (1991).
[18] R. W. G. Wyckoff, *Crystal Structures* (Interscience, New York, 1960).
[19] G. E. Rush, A. V. Chadwick, I. Kosacki, and H. U. Anderson, J. Phys. Chem. B **104**, 9597 (2000).